

Swift **BAT**, *Fermi* **LAT**, and the **Blazar Sequence**

R. M. Sambruna

NASA/GSFC, Code 662, Greenbelt, MD 20771

D. Donato

NASA/GSFC, Code 661, Greenbelt, MD 20771

M. Ajello

*SLAC National Laboratory and Kavli Institute for Particle Astrophysics and Cosmology,
2575 Sand Hill Road, Menlo Park, CA 94025, USA*

L. Maraschi

INAF - Osservatorio Astronomico di Brera, V. Brera 28, I-20100 Milano, Italy

J. Tueller, W. Baumgartner, G. Skinner, C. Markwardt, S. Barthelmy, N. Gehrels

NASA/GSFC, Code 661, Greenbelt, MD 20771

R.F.Mushotzky

NASA/GSFC, Code 662, Greenbelt, MD 20771

ABSTRACT

Using public *Fermi* LAT and *Swift* BAT observations, we constructed the first sample of blazars selected at both hard X-rays and gamma-rays. Studying its spectral properties, we find a luminosity dependence of the spectral slopes at both energies. Specifically, luminous blazars, generally classified as FSRQs, have *hard* continua in the medium-hard X-ray range but *soft* continua in the LAT gamma-ray range (photon indices $\Gamma_X \lesssim 2$ and $\Gamma_G \gtrsim 2$), while lower luminosity blazars, classified as BL Lacs, have opposite behavior, i.e., *soft* X-ray and *hard* gamma-ray continua ($\Gamma_X \gtrsim 2.4$ and $\Gamma_G < 2$). The trends are confirmed by detailed Monte Carlo simulations explicitly taking into account the observational biases of both instruments. Our results support the so-called “blazar sequence” which was originally based on radio samples of blazars and radio luminosities. We also argue that the X-ray-to-gamma-ray continua of blazars may provide independent insights into the physical conditions around the jet, complementing/superseding the ambiguities of the traditional classification based on optical properties.

Subject Headings: Galaxies: active — galaxies: radio — galaxies: individual — X-rays: galaxies

1. Introduction

Our study of the high-energy extragalactic sky has been propelled forward thanks to the launch in June 2008 of the *Fermi* Gamma-ray Observatory. After only three months of operations the LAT experiment already detected over a hundred sources at $\gtrsim 10\sigma$, of which 99 are blazars and 2 are radio galaxies (Abdo et al. 2009a). The publication of the LAT Bright Source Catalog (Abdo et al. 2009a) prompted a few studies of the statistical properties of gamma-ray selected blazars (Ghisellini, Maraschi, & Tavecchio, 2009; Kovalev et al. 2009; Lister et al. 2009), as well as of their Spectral Energy Distributions (SEDs; see e.g., Abdo et al. 2009c).

One of the hot debates concerning blazar SEDs is the general validity of the so-called “blazar sequence”. According to the latter, when blazar SEDs are arranged in order of decreasing bolometric luminosity their shapes change in an orderly fashion, with the synchrotron and Compton peaks moving to higher energies in accord (Fossati et al. 1998). It is important to stress that the original blazar sequence was discovered using blazar samples selected from the radio and X-rays, but binned according to radio luminosity only (Fossati et al. 1998), leading to biases (Padovani 2007; but see Ghisellini & Tavecchio 2008, Maraschi et al. 2008 for a rebuttal). Moreover the gamma-ray data available at the time were scarce (Maraschi & Tavecchio 2001). A replica of the sequence at gamma-rays was recently found by Ghisellini, Maraschi, & Tavecchio (2009) based on the *Fermi* 3 months blazar list. They found that more luminous gamma-ray sources have softer LAT spectra, with the BL Lac and FSRQ populations occupying neatly separated regions. The dividing luminosity was interpreted in terms of a critical accretion rate, $\sim 10^{-2}$ the Eddington one, regulating the transition from efficient accretion in FSRQs to inefficient accretion in BL Lacs (Ghisellini, Maraschi, & Tavecchio 2009).

With its large field of view, nearly continuous sky coverage, and improved sensitivity (35 mCrab in 2 ks and ~ 1 mCrab in 36 months in 14.5–195 keV) the BAT experiment onboard *Swift* is an important complement to *Fermi* for blazar science. Its sensitivity to flaring hard X-ray sources, and to quiescent emission of blazars out to $z = 4$, makes it ideal for studying the high-energy SEDs in tandem with the LAT. The BAT has already performed a 3 year survey of the sky, detecting 38 blazars at higher galactic latitudes (Ajello et al. 2009); using these data we constructed the first high-energy selected sample of blazars detected at both hard X-ray and GeV gamma-rays. Here we study the high-energy SEDs of this sample combining the BAT and LAT spectra, showing that the main result of the spectral sequence - a luminosity dependence of the high-energy peak - is independently recovered.

This paper is structured as follows. § 2 describes the sample. § 3 presents the results of the BAT-LAT comparison, and § 4 their interpretation. A concordance cosmology with

$H_0 = 71 \text{ km s}^{-1} \text{ Mpc}^{-1}$, $\Omega_\Lambda=0.73$, and $\Omega_m=0.27$ (Spergel et al. 2003) is adopted. Photon indices are defined as $\Gamma = \alpha - 1$, where the energy index α is such that $F_\nu \propto \nu^{-\alpha}$. Luminosities were K-corrected according to the equation $L_K=L/(1+z)^{(1-\alpha)}$.

2. Sample and Data

The sample was derived primarily from the list of 99 blazars at $|b| > 10^\circ$ detected with the LAT at more than 10σ in the first 3 months of operations during August 4 – October 8, 2008 (Abdo et al. 2009a). To increase the sample size for intersection with the BAT sample, we also considered the list of detected extragalactic sources which include those on the Galactic plane as well (Abdo et al. 2009b). Absorption at X-rays is not a concern, as the BAT operates at energies $\gtrsim 15 \text{ keV}$ and is thus unaffected by typical column densities $N_H < 10^{24} \text{ cm}^{-2}$.

BAT performed a 3 year survey of the sky detecting 38 blazars above a significance of 5σ at $|b| > 10^\circ$. As noted in Ajello et al. (2009), only 12 of the blazars detected by BAT above 5σ were also detected by LAT. We thus searched the BAT all-sky image for statistical fluctuations above the 3σ level at the positions of the 99 LAT blazars. This produced a list of 22 LAT blazars which are also detected by BAT above the 3σ level. The probability that at least one of these $\geq 3\sigma$ fluctuations is given by chance is only 0.1. There is no intrinsic difference between the samples of BAT sources selected above 3σ and 5σ which are common to the LAT dataset. Indeed, the mean redshift of the 12 and 22 BAT sources (selected respectively above 5σ and 3σ) is 0.75 and 0.73 being the dispersion of both distributions 0.77. The average flux of the sample decreases from $6.7 \times 10^{-12} \text{ erg cm}^{-2} \text{ s}^{-1}$ to $5.1 \times 10^{-12} \text{ erg cm}^{-2} \text{ s}^{-1}$.

Thus, the final sample used in this work includes a total of 22 blazars, of which 10 are BL Lacs and 12 are FSRQs. The confirmed TeV sources among the BL Lacs are four - Mrk 421, Mrk 501, 1ES 1959+650, and BL Lac itself. We stress that this is a *hard X-ray/gamma-ray selected* sample, and therefore *unbiased toward the radio and optical properties*.

The data used for this work are derived from the spectral analysis. For the BAT, spectra were extracted according to the procedure detailed elsewhere (Ajello et al. 2009, Tueller et al. 2008; consistent with each other) and fitted with single power law models, deriving photon indices Γ_X and broad-band fluxes integrated in the 14–195 keV energy range. A single power law provides a good fit to the BAT spectra of all sources. For the LAT, Table 3 in Abdo et al. (2009a) provides the LAT photon index Γ_G and fluxes derived in various ways; we choose to use the flux derived by a power-law fit in the energy range 0.2–100 GeV. Results do not

change if fluxes derived with other methods are used instead.

For 1ES 0033+59.5 and PKS 1830–21, only multiband fluxes are provided in Abdo et al. (2009b). We used these fluxes to derive a crude estimate of the spectral index, which in both cases turned out to be > 2 . As a sanity check, we repeated this exercise for all the sources in common between Abdo et al. (2009a) and (2009b), and compared the photon index derived from the flux ratios to the photon index Γ_G , finding good agreement within 10% especially for $\Gamma_G \lesssim 2$. This gives us confidence that the slopes from the flux ratios are a sensible approximation of the LAT continua for the two sources.

Finally, the BAT survey overlaps with the 3-months of the LAT operations, and thus contains simultaneous data. While in principle it should be possible to consider only the BAT data segments overlapping in time with the LAT data, in practice this is not feasible due to the limited sensitivity of the detector. The fluxes and spectra analyzed here thus represent average states integrated over the whole 36 months of the BAT survey. For a more detailed discussion of non-simultaneous data and the blazar sequence, see Ghisellini et al. (2009) and references therein.

3. Results

First, we examine the redshift distribution of the sources to ensure that it is randomly drawn and thus representative of the whole population. Figure 1 shows the distribution in redshift of the sources (shaded histogram) compared to the total LAT blazar population from the 3-months survey. There is no difference between the two histograms, as confirmed by a Kolmogorov-Smirnov (KS) test, indicating no bias in distance/volume distribution for the GeV sources. Both LAT and BAT are sensitive to blazar emission up to large redshifts, because of intrinsic beaming of the jet radiation (Ajello et al. 2009). In addition, while the selection of the sample based on the large TS value in the LAT data favors bright/flaring sources, Figure 1 stresses that there is no bias towards to most *luminous* blazars.

Figure 2 shows the plot of the LAT and BAT spectral indices. FSRQs are plotted with open circles, while BL Lacs with open triangles. The BL Lacs detected at TeV energies are plotted with starred triangles. 1ES 0033+59.5 and PKS 1830–21 are plotted in dotted lines (see § 2). In Figure 2 blazars segregate in two distinct regions of the diagram, one with $\Gamma_X \lesssim 2$ and $\Gamma_G \gtrsim 2$, and the other with $\Gamma_X \gtrsim 2.4$ and $\Gamma_G < 2$. The former region, with *soft* gamma-ray but *hard* X-ray continua, is populated by FSRQs and some BL Lacs; the latter, with *hard* gamma-ray but *soft* X-ray continua, contains only BL Lacs, including 3 confirmed TeV sources. These soft X-ray continuum BL Lacs are also known as HBLs -

High Energy-peaked BL Lacs. A KS test confirms that FSRQs and HBLs are distributed differently both in Γ_G and Γ_X at 3σ or more.

The BL Lac 1ES 0033+59.5, marked in the Figure, is an outlier being positioned in the region of steep BAT spectra despite its LAT continuum similar to other BL Lacs. Large X-ray variability affects its location. To showcase this, we plotted its position in the diagram as implied by a previous *BeppoSAX* broad-band measurement that gave a flatter X-ray continuum than the BAT (Costamante et al. 2001; Donato et al. 2004).

Interestingly, within the $\Gamma_X \lesssim 2$ and $\Gamma_G \gtrsim 2$ region there is a hint for a further separation in Γ_G between FSRQs and BL Lacs. The KS test probability that the two distributions are drawn from the same parent one is 6.7×10^{-4} . These “intermediate” BL Lacs are also distributed differently than HBLs, in both spectral indices.

Since FSRQs are distant and luminous at GeV gamma-rays while BL Lacs tend to be closer and fainter (e.g., Ghisellini et al. 2009), Figure 2 suggests a relationship between slopes and luminosities as well. A trend between Γ_G and the GeV luminosity is already known (Ghisellini et al. 2009). Here we add the BAT data to show how the shape of the high-energy component, from X-ray to gamma-rays, changes with gamma-ray luminosity.

Figure 3a (top panel) shows the plots of the LAT photon index, Γ_G , versus the gamma-ray luminosity while in Figure 3b (bottom panel) we show the plot of the BAT spectral index, Γ_X , versus the BAT luminosity. Figure 3a is the well-known correlation from Abdo et al. (2009a) and Ghisellini et al. (2009), showing how the LAT slope steepens going from lower-luminosity BL Lacs to higher-luminosity FSRQs. The new piece of information added here is the trend in the bottom panel, that shows an opposite trend for Γ_X to harden with increasing luminosity.

There are two outlier BL Lacs in Figure 3, with luminosities $> 10^{46}$ erg s $^{-1}$ and continuum slopes similar to FSRQs: PKS 0537–441 and PKS 0426–380. The former, at $z=0.892$, is variously classified as a FSRQ/BL Lac due to its variable broad optical lines (Maraschi et al. 1985). Thus this source can be considered a transition object where a broad line region is present but the emission lines are swamped at times by the variable non-thermal continuum. Similarly, a broad H α line was detected on one instance in BL Lac itself, the prototype of the class (Vermeulen et al. 1995), which in Figure 2 is located in the region of the intermediate group (starred triangle). The second discrepant object is PKS 0426–380 at $z=1.11$. In fact its redshift was derived from a broad MgII line in emission, while absorption redshifts due to intervening galaxies had been measured previously (Heidt et al. 2004). Thus also for PKS 0426–380, a radio-selected BL Lac from the Stickel et al. (1991) sample, the BL Lac classification is questionable.

The results of Figure 3 are recast in different visual format in Figure 4. Here we show the high-energy SEDs of the sources grouped in five bins of increasing X-ray luminosity, following the procedure of Fossati et al. (1998) at radio. Plotted in Figure 4 are the average BAT and LAT SEDs and their 1σ deviations. The Figure shows the shift of the SED shape with the luminosity.

To assess the possibility of biases introduced by the limited sensitivity of the instruments, we performed detailed Monte Carlo simulations, assuming random distributions of gamma-ray luminosities, and gamma-ray and X-ray spectral indices (see Appendix). The probability of obtaining by chance the plots in Figure 3a-b is 3.4%, i.e., the probability that the observed trends between the luminosity and the slopes at high energies are intrinsic is 96.6%. We thus conclude that there is a trend in Figure 3 and 4 for the shape of the high-energy SED to change with gamma-ray luminosity, specifically, its peak shifts forward with decreasing luminosity.

4. Discussion and Conclusions

We have examined the hard X-ray and gamma-ray spectral properties of a sample of blazars selected at high energies. Our main observational findings, summarized by Figures 2 and 3, are as follows: 1) FSRQs and HBLs segregate apart in the shape of their high-energy SEDs. FSRQs have soft slopes in the gamma-ray band (100 MeV–300 GeV) and hard slopes in the X-ray band (15–195 keV), and HBLs have hard continua at gamma-rays and soft continua at X-rays. The remaining BL Lacs form a transition group between the two; and 2) this division in slopes depends on gamma-ray luminosity. In other words, the hard X-ray and gamma-ray spectra jointly can univocally determine the location of the high-energy peak in the SED.

We interpret these results in the context of the double-humped blazar SEDs mentioned in § 1. First, it is important to visualize where the sensitivity energy ranges of the BAT and LAT are located with respect to the SEDs. In FSRQs, the BAT energy range covers the region where the inverse Compton emission starts to emerge, while the LAT spans the Compton peak and above; thus, we expect to observe hard X-ray spectra and soft GeV spectra in this class of blazars. In HBLs, however, it is the steep high-energy tail of the synchrotron emission that fills the BAT energy band, yielding *soft* BAT spectra. In these sources the Compton peak is at TeV energies, beyond the LAT sensitivity range; thus, at MeV-GeV energies this component is still rising, and *hard* LAT spectra are expected. Figure 2 shows that, indeed, sources with hard BAT spectra inevitably have soft gamma-ray spectra, and vice-versa.

According to Figures 3 and 4, the position of the Compton peak depends on the gamma-ray luminosity. The more gamma-ray luminous blazars have steeper Γ_G and flatter Γ_X , i.e., their Compton peak tends to fall between MeV and GeV energies. On the contrary, less luminous GeV sources exhibit the opposite behavior, i.e., they have Compton peaks beyond the LAT band. We have thus recovered, at the higher energies and with a *high-energy selected blazar sample*, the main result of the blazar sequence – the luminosity dependence of the peak energy position. This adds to the recent evidence from the gamma-rays only (Ghisellini et al. 2009).

Variability will not change significantly the position of FSRQs and most LBLs in Figure 2. While all sources vary in flux, the most dramatic continuum shape variations so far have been observed above the synchrotron peak, i.e., for the X-ray spectra of HBLs. These objects are expected to move horizontally in the $\Gamma_X \gtrsim 2$ region in the majority of cases, as shown by 1ES0033+595. Extreme BL Lacs, which can reach $\Gamma_X \sim 1$, are the only exception but only a few examples are known so far (Costamante et al. 2001).

Another result of Figure 2 is that a subgroup of objects traditionally classified as BL Lacs are located nearby FSRQs but completely set apart from HBLs. These sources are characterized by similar X-ray continua as powerful quasar-like blazars, $\Gamma_X \sim 1.8$, but flatter gamma-ray slopes, $2.1 < \Gamma_G < 2.3$. Among these sources we find objects like ON 325 and BL Lac itself, known for their “intermediate” properties. For example, BL Lac has a concave 0.5–10 keV spectrum (Tanihata et al. 2000) which is interpreted as the crossing of the synchrotron and Compton components (as predicted by the sequence for mid luminosities), and which occasionally display broad emission lines in the optical (Vermeulen et al. 1995). On the contrary, none of the HBLs was ever observed to exhibit broad optical lines.

Our idea is that the phenomenological definition of BL Lacs, based on upper limits to the emission line equivalent width (e.g., Angel & Stockman 1980) leads to a “hybrid” class, composed of two subgroups: sources that intrinsically lack broad emission line regions (the *bona fide* BL Lacertae objects) and sources that, like BL Lac itself, occasionally exhibit broad Balmer lines. In the lineless objects the accretion flow is largely sub-Eddington ($\dot{m} \leq 10^{-2}$) and therefore radiates inefficiently so that an optically thick disk does not form and the broad line region is absent. They are TeV sources and are unified with FRI radio galaxies according to unification schemes.

The objects of the second group are classified differently depending on the epoch of observation, appearing as quasar-like during low states of the jet non-thermal continuum, and BL Lacertae-like when the jet emission is in a high state and swamps the line emission. In these objects the accretion flow is relatively weak, but above the limit for inefficient accretion ($\dot{m} \geq 10^{-2}$) so that a broad line region is formed but with sub-Eddington luminosity. Thus,

it is easier for the non-thermal continuum to wash out the emission lines in high states. The presence of such broad line region affects the jet high-energy spectrum, though less strongly than for ordinary FSRQs: the radiative losses due to IC scattering of the relativistic electrons in the jet on the BLR photons can be responsible for a lower peak energy of the electrons and therefore for a Compton peak at intermediate energies, thus accounting for an intermediate gamma-ray spectral index (Celotti & Ghisellini 2008). The parent population of these occasional line emitters should correspond to intermediate FRI/II morphologies (Kollgaard et al. 1991).

From this perspective, Figure 2 shows that the shape of the high-energy emission offers an independent mean to probe the astrophysical conditions at the blazar nucleus. The hard X-ray through gamma-ray continuum carries information on the nuclear ambient where the jet forms and radiates, being sensitive to the energy density of photons in and around it, and can be read as a proxy for the accretion rate (in Eddington units) onto the black hole. This holds on a long-term "average". Clearly large flares in the jet involving events of increased particle acceleration/injection can produce large variations in the high-energy spectrum. Detailed spectral modeling is required for a more quantitative assessment of the fundamental properties (jet power, accretion rate, and mass) of these blazars (Ghisellini & Tavecchio 2008).

In conclusion, using a high-energy selected blazar sample we have recovered one of the main tenets of the so-called blazar sequence – the luminosity dependence of the position of the Compton peak. The high-energy emission appears as a promising tool to differentiate among blazar flavors in an unbiased way. From this perspective, we look forward to many more years of BAT and LAT synergy.

We thank the BAT and LAT teams for making these observations possible. Interesting conversations with C. Dermer and M. Kadler in earlier phases of the work are also acknowledged. An anonymous referee raised some good points in his/her report that stimulated additional work.

5. Appendix

As can be seen in Figure 7 of Abdo et al. (2009a), the LAT is inherently biased towards steep-spectrum/bright sources. One can thus wonder whether these biases affect the trends between spectral index and luminosity observed in Figure 3. On the other hand no strong selection effect has been reported for BAT (e.g., Ajello et al. 2008, Tueller et al. 2009).

In order to test this possibility, we performed a detailed Monte-Carlo study explicitly including the sensitivity limits of the detectors. We start by recasting Figure 3a-b into a unified plot by plotting the difference of the BAT and LAT indices, $\Delta\Gamma = \Gamma_X - \Gamma_G$, versus the luminosity for simplicity of analysis; the result is shown in Figure 5. As expected, more luminous sources have more negative $\Delta\Gamma$. Performing a linear correlation analysis we find a coefficient of variation, i.e., the squared of the linear correlation coefficient, of 0.57 between $\Delta\Gamma$ and the luminosity in Figure 5.

The main goal of the simulation is to verify whether the trend observed in Figure 5 is real or due to instrumental biases. The blazar sequence manifest itself as a correlation between luminosity and spectral shape (in our case photon index). The lower the luminosity, the flatter the photon index (i.e. the high-energy peak shifts at larger energies) while the larger the luminosity the steeper the index (e.g., $\Gamma_G > 2.3$). In this set of Monte Carlo simulations we aim at generating samples of sources where luminosity and indices are uncorrelated, corresponding to the case in which the blazar sequence does not exist, and a-posteriori applying the selection effects of LAT. If out of a large number of simulations we found that the correlation index is $\gtrsim 0.57$ for a significant number of cases, the trend in Figure 5 would be produced, very likely, by instrumental effects.

For this set of simulations we drew random sources from the flux, index, and redshift distributions observed for the LAT sources (see Abdo et al. 2009a). We remark that the distributions are sampled independently in order to study whether the LAT biases would a-posteriori introduce any correlation. Moreover, in order to be as accurate as possible, the sources were not drawn from a model fit to the observed distributions (e.g., a Gaussian fit to the index or redshift distribution), but rather from the raw observed distributions themselves. From a physical point view, in this sample low-luminosity hard FSRQs and very luminous high-redshift BL Lac objects exist in comparable numbers. We then rejected all those sources which given a certain flux would have a photon index too steep to be detected by LAT (see Fig.7 of Abdo et al. 2009a). To each LAT source we coupled a BAT photon index extracted independently from the observed distribution of BAT photon indices, the latter described by a Gaussian centered at $\Gamma_{BAT} = 1.86$ and with dispersion 0.46. Then, we grouped the sources in samples counting 21 objects and produced the corresponding distribution shown in Figure 5. Only 34 out of 1000 plots have a correlation index larger than 0.57, implying that the probability of observing by chance Figure 5 correlation is only 3.4%.

In a sense, LAT cannot observe (if they existed) low luminosity FSRQs, but can easily detect luminous BL Lac objects. If that were the case (i.e., there are BL Lacs at high redshifts), no correlation would exist between the LAT luminosity and difference between

the BAT and the LAT photon indices. While it is not within the scope of this paper to discuss the existence of BL Lac objects at very high redshift we conclude noting that these objects are currently not present in the LAT datasets although not all BL Lac objects have a redshift measurement available at the moment (see Abdo et al. 2009a).

REFERENCES

- Abdo, A. A. 2009a, *ApJ*, 700, 597
- Abdo, A. A. 2009b, *ApJS*, 183, 46
- Abdo, A. A. 2009c, *ApJ*, 697, 934
- Angel, J.R.P. & Stockman, H.S. 1980, *ARA&A*, 18, 321
- Ajello, M. et al. 2009, *ApJ*, 699, 603
- Celotti, A. & Ghisellini, G. 2008, *MNRAS*, 385, 283
- Costamante, L. et al. 2001, *A&A*, 371, 512
- Donato, D. et al. 2004, *A&A*, 375, 39
- Fossati, G., Maraschi, L., Celotti, A., Comastri, A., & Ghisellini, G. 1998, *MNRAS*, 299, 433
- Ghisellini, G., Maraschi, L., & Tavecchio, F. 2009, *MNRAS*, 396, L105
- Ghisellini, G. & Tavecchio, F. 2008, *MNRAS*, 287, 1669
- Heidt, J. et al. 2004, *A&A*, 418, 813
- Kollgaard, R. I., Wardle, J. F. C., Roberts, D. H., Gabuzda, D. C. 1991, *AJ*, 104, 1687
- Kovalev, Y.Y. et al. 2009, *ApJ*, 696, L17
- Lister, M.L. et al. 2009, *ApJ*, 696, L22
- Maraschi, L., Foschini, L., Ghisellini, G., Tavecchio, F., & Sambruna, R.M. 2008, *MNRAS*, 391, 1981
- Maraschi, L. & Tavecchio, F. 2001, *ASPC*, 227, 40
- Maraschi, L., Treves, A., Schwartz, D. A., & Tanzi, E. G. 1985, *ApJ*, 294, 615
- Padovani, P. 2007, *Ap&SS*, 309, 63
- Spergel, D. N., et al. 2003, *ApJS*, 148, 175
- Stickel, M., Fried, J. W., Kuehr, H., Padovani, P., & Urry, C. M. 1991, *ApJ*, 374, 431
- Vermeulen, R.C. et al. 1995, *ApJ*, 452, L5

Tanihata, C. et al. 2000, ApJ, 543, 124

Tueller, J., Mushotzky, R. F., Barthelmy, S., Cannizzo, J. K., Gehrels, N., Markwardt, C. B.,
Skinner, G. K., & Winter, L. M. 2008, ApJ, 681, 113

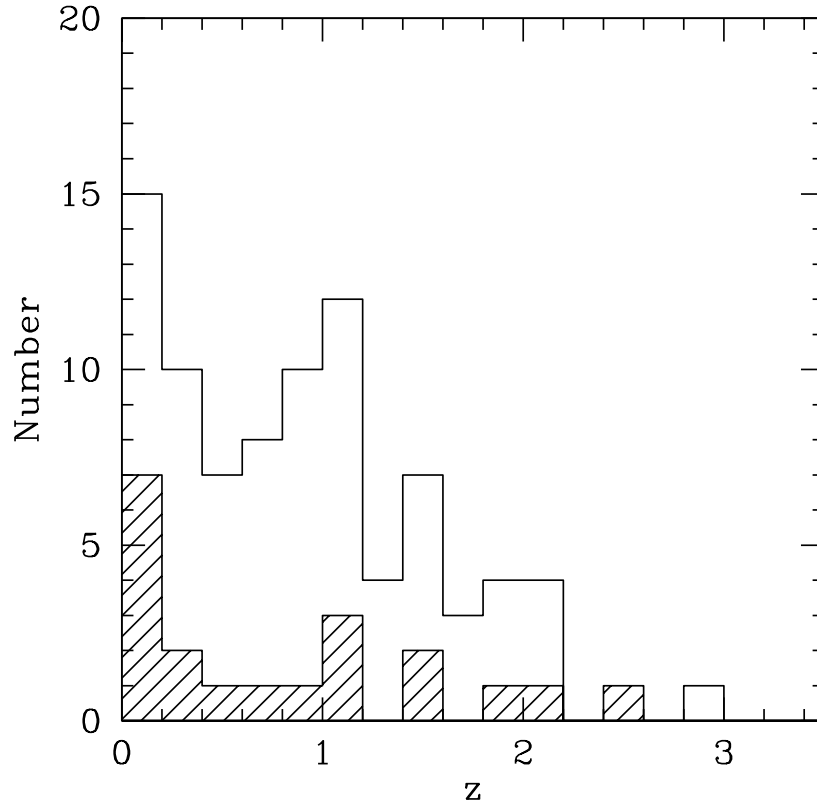


Fig. 1.— Distributions of the redshifts of the blazars detected with both the BAT and LAT (shaded histogram) and of the LAT 3 months blazar list (Abdo et al. 2009a).

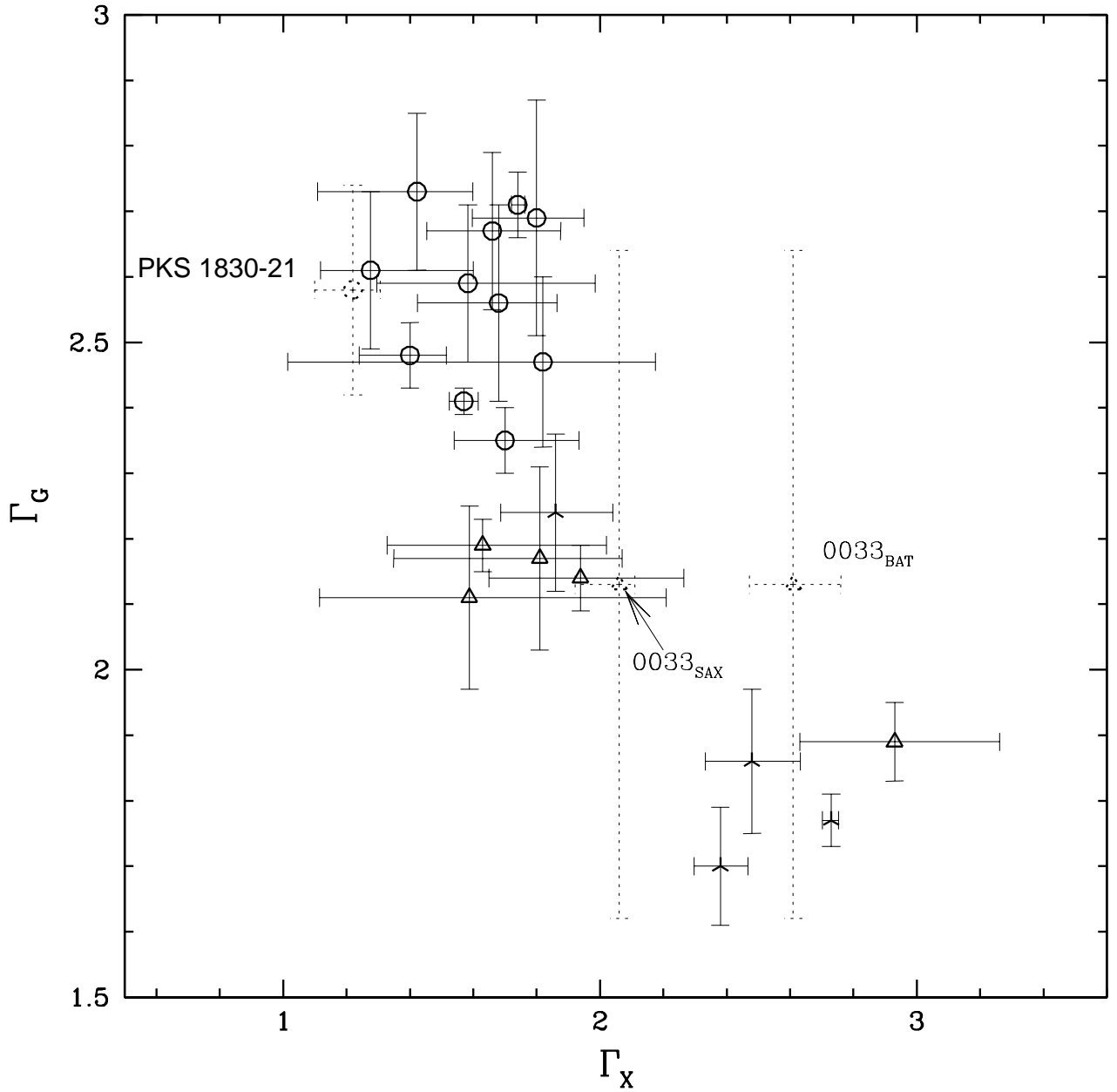


Fig. 2.— Plot of the LAT photon index, Γ_G , versus the BAT photon index, Γ_X , for the blazars detected by both instruments (see text). Open circles are FSRQs, open triangles are BL Lacs, and starred triangles are BL Lacs detected at TeV energies. Errorbars are 1σ .

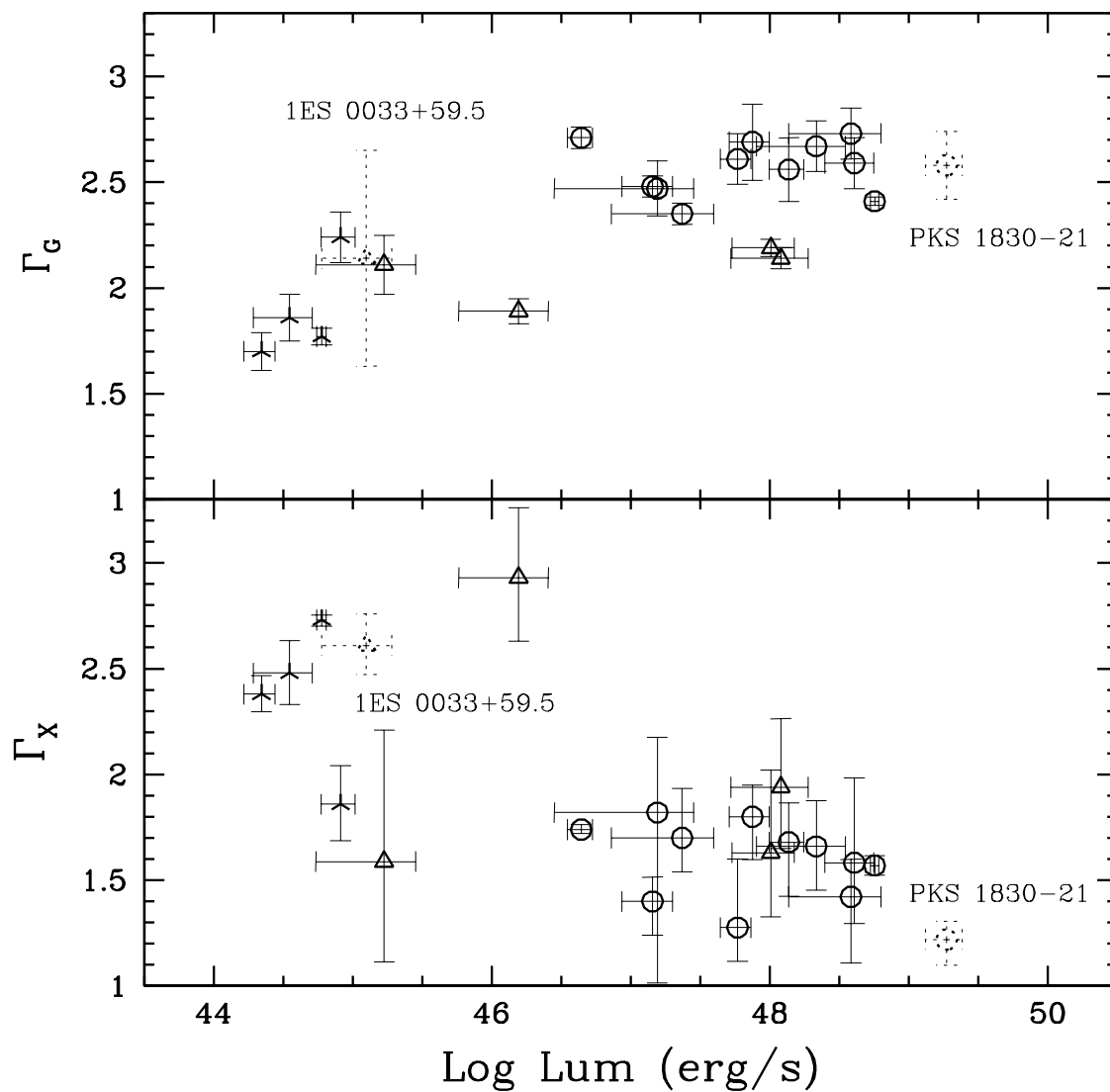


Fig. 3.— (a, *Top*) Plot of the LAT photon index versus the LAT luminosity (from Abdo et al. 2009, Ghisellini et al. 2009), showing a trend of steeper slope for more luminous sources. (b, *Bottom*) Plot of the BAT photon index versus the BAT luminosity showing the opposite behavior than in (a), i.e., a flatter X-ray continuum for increasing luminosity. Open circles are FSRQs, open triangles are BL Lacs, and starred triangles are BL Lacs detected at TeV energies. Errorbars are 1σ .

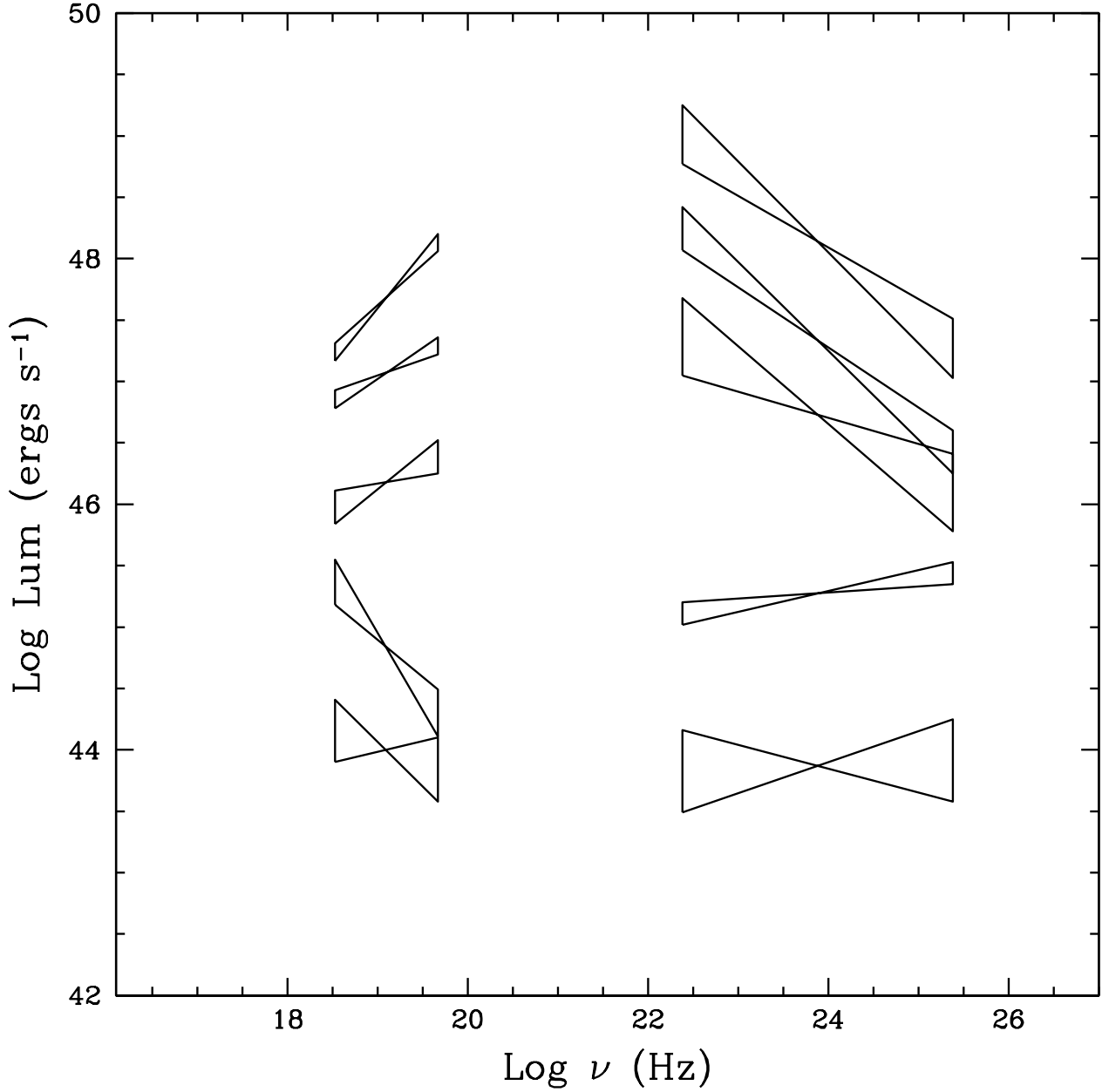


Fig. 4.— Plot of the BAT and LAT average continua in bins of BAT luminosity (see text). This shows that the IC peak shifts to lower energies with increasing luminosity, recovering the Fossati et al. (1998) “blazar sequence”. Errorbars are 1σ .

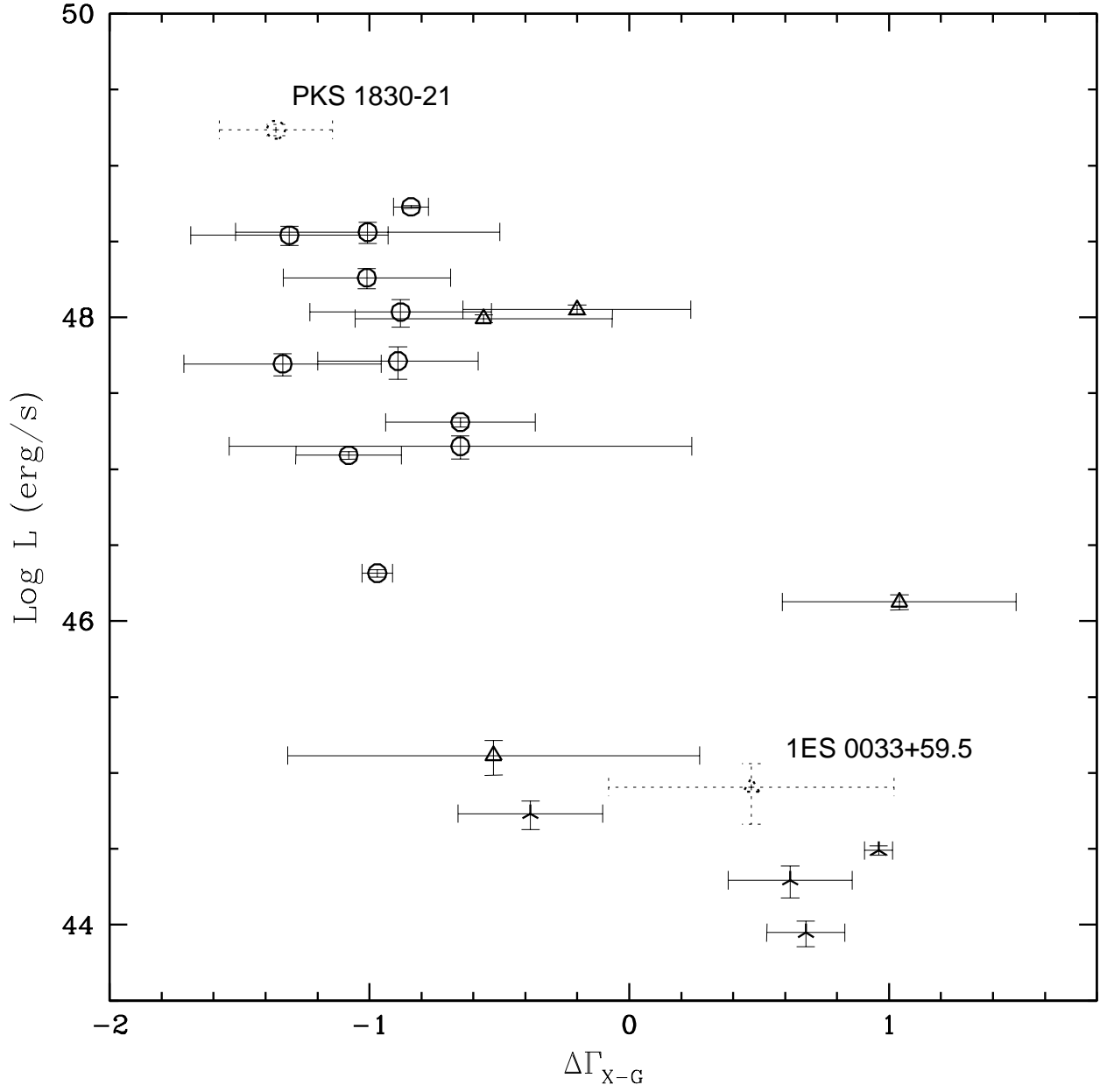


Fig. 5.— Plot of the difference between the BAT and LAT slopes versus the LAT luminosity. Open circles are FSRQs, open triangles are BL Lacs, and starred triangles are BL Lacs detected at TeV energies. Errorbars are 1σ .